MODIFIED PRESSURE SYSTEM FOR IMAGING EGG CRACKS

K. C. Lawrence, S. C. Yoon, D. R. Jones, G. W. Heitschmidt, B. Park, W. R. Windham

ABSTRACT. *One aspect of grading table eggs is shell checks or cracks. Currently, USDA voluntary regulations require that humans grade a representative sample of all eggs processed. However, as processing plants and packing facilities continue to increase their volume and throughput, human graders are having difficulty matching the pace of the machines. Additionally, some plants also have a problem with micro-cracks that the graders often miss because they are very small and hard to see immediately post-processing but grow and become readily apparent before they reach market. An imaging system was developed to help the grader detect these small micro-cracks. The imaging system utilized one image captured at atmospheric pressure and a second at a slight negative pressure to enhance the crack and make detection much easier. A simple image processing algorithm was then applied to the ratio of these two images, and the resulting image, containing both cracked and/or intact eggs were color-coded to simplify identification. The imaging system was capable of imaging 15 eggs in about 0.75 s, and the algorithm processing took about another 10 s. These times could easily be reduced with a compiled program specifically written for the application. In analyzing 1000 eggs, the system was 99.6% accurate overall with only 0.3% false positives, compared to 94.2% accurate overall for the human graders with 1.2% false positives. An international patent on the system has been filed, and further automation of the system is needed.*

Keywords. *CCD camera, Cracks, Image processing, Machine vision, Negative pressure, Shell eggs, Vacuum.*

The majority of table eggs in the U.S. are processed with automated sorting, grading, and packing machines and, as in most industries, the trend is towards higher volume and faster processing speeds. Advances in modern poultry egg grading machines have resulted in throughputs of up to 120,000 eggs per hour, making it hard for the human graders, who only grade a small portion of the eggs, to keep up. Furthermore, since grading of table eggs is done on a voluntary basis and is administered by the USDA Agricultural Marketing Service (AMS) (USDA, 2000), it is driven by the demands of the customer, with most of the consumer market and many of the large food conglomerates requiring their eggs to be certified or "shielded" (i.e., the eggs receive the USDA grade shield for quality attributes). Plants that operate under the USDA shield are required to have a certain portion of their eggs graded by AMS human graders or their assigned representative (one out of 75 cases). For a plant operating at 500 cases per hour, that corresponds to about 11 eggs per minute. This shielding program also ensures that certain production and processing parameters have been met. In the largest plants, the limiting factor for the processing speed is becoming the human grader, leading to a need for a second grader. Since this program is voluntary, the plant has to pay for the service, which can become cost-prohibitive when two graders must work a processing line. Furthermore, in addition to an increase in the number of eggs needing grading, there is also a trend in which more egg shells are exhibiting micro-cracks. Micro-cracks are very minute, hairline cracks that often cannot be detected by the graders at the time of processing. These micro-cracks can be caused by numerous conditions but tend to be more prevalent in in-line facilities operating at higher line speeds. Then, as eggs with micro-cracks cool in storage, the thermal stresses on the shell cause these micro-cracks to expand and enlarge so that the overall percentage of cracked eggs is sometimes greater than what is allowed by USDA guidelines. For example, USDA Grade A eggs cannot contain more than 5% cracked eggs leaving the packing line (USDA, 2000). Thus, there is a need for a system to aid the graders in detecting these micro-cracks.

A few years ago, DeKetelaere et al. (2004) published an extensive review of non-destructive measurements of egg quality. They reported that methods for egg crack detection could be divided into three categories: mechanical, machine vision, and vibration analysis. Mechanical techniques could be further divided into destructive and non-destructive. Obviously, destructive methods were not suitable for grading and none of the non-destructive methods had better than moderate correlations with egg-shell cracks.

Vibration analysis methods have been developed to rapidly detect eggshell cracks, and several of the methods have been patented and commercialized. Of particular interest was a piezo-sensor based system that had a crack detection rate of 70% to 85% when the egg was impacted with the weighted piezo sensor between 24 and 32 times at various locations (DeKetelaere et al., 2004; Bliss, 1973). An alter-

Submitted for review in August 2008 as manuscript number IET 7654; approved for publication by the Information & Electrical Technologies Division of ASABE in June 2009. Presented at the 2008 ASABE Annual Meeting as Paper No. 084030.

Mention of company or trade names is for description only and does not imply endorsement by the USDA.

The authors are **Kurt C. Lawrence, ASABE Member Engineer,** Research Leader, **Seung Chul Yoon, ASABE Member Engineer,** Research Electronics Engineer, **Deana R. Jones,** Research Food Technologist, **Gerald W. Heitschmidt,** Image Analyst, **Bosoon Park, ASABE Member Engineer,** Research Agricultural Engineer, and **William R. Windham,** Research Physiologist, USDA-ARS Russell Research Center, Athens, Georgia. **Corresponding author:** Kurt C. Lawrence, USDA-ARS Russell Research Center, P.O. Box 5677, Athens, GA 30604-5677; phone: 706-546-3527; fax: 706-546-3607; e-mail: kurt.lawrence@ars.usda.gov.

  ISSN 0001–2351

nate approach was to have the egg impact a stationary sensor and measure the frequency response of the subsequent vibrations. This method required only four impacts and resulted in a 90% crack-detection accuracy with a false rejection rate of 0.5% (DeKetelaere et al., 2004; Bliss, 1973; Coucke, 1998). Other vibrational methods were reported, but none were as accurate at detecting cracks and all had false rejections (false positives) greater than 1%. DeKetelaere et al. (2004) recommended that for comparison purposes, crack detection accuracy should be reported with no more than a 1% false rejection level.

The third method of crack detection used a machine vision system to mimic the visual inspection of a crack. Some of the earliest work used a monochromatic camera imaging an egg with incandescent light transmitted through the egg and relied on various image-processing algorithms to identify the crack from other shell features (Elster and Goodrum, 1991; Goodrum and Elster, 1992). These methods resulted in a 96% accuracy with a 5.6% false rejection rate on cracks of substantial size but took 25 s to analyze a single egg. Later work resulted in 90% accuracy at a much faster inspection rate. A novel method for detecting eggshell cracks was proposed by Lin et al. (2001). They used a compression chamber to apply pressure to an egg during which time an image was captured. The pressure was released while a second image was captured. This second image was used to help identify the crack. They reported an accuracy of 80% and 86% for cracked and sound eggs, respectively.

From the literature review, the best results for egg-crack detection were slightly over 90% with a 0.5% false rejection rate (DeKetelaere et al., 2000). Closer examination of the data indicated the researchers used two methods to select cracked eggs, both of which were from naturally occurring causes (not artificially cracked). The first method collected 360 eggs after they were graded with a commercial grading system. These eggs were then graded a second time by two human graders, and 23 of 360 eggs were found to be cracked. With this method, most of the cracks were considered to be small, hairline cracks. The second set of eggs was collected prior to the commercial grading system and had 101 of 287 eggs cracked. Eggs collected at this point would typically include eggs with larger cracks. For the first dataset, the accuracy of egg crack detection was 87%, while the false rejection rate was 0.6%, excluding eggs with body checks and loose air cells. Adding these eggs increased the false rejection rate. Thus, in trying to develop a new method to detect micro-cracks, these accuracies should be bettered in a new system.

In discussions with egg researchers, graders, and producers, it was observed that human graders used two basic methods to identify egg cracks. In the first technique, graders gently tapped, or "belled," two eggs together and listened for a "dull" sound. This technique relied on the acoustic properties of the eggs as described above (DeKetelaere et al., 2000). The second method was simply to visually inspect the egg for a crack. If there was a feature that looked like it might be a crack and/or the grader had heard the indicative sound of a cracked egg, then they would press and/or squeeze the egg to help confirm the presence of a crack. Recent research with an imaging system tried to emulate this process (Lawrence et al., 2008). First, numerous attempts were made to use, develop, and/or combine imaging processing algorithms to detect the cracks. Although successful at identifying cracks, the algorithms also detected numerous non-crack shell features, resulting in numerous false positives (Lawrence et al., 2008). Thus, the researchers concluded that a method to enhance the crack was needed. Furthermore, attempts to use hyperspectral imaging to find spectral differences between egg-shell cracks and other egg-shell features were also unsuccessful.

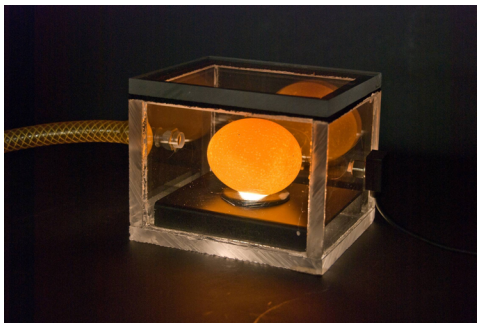

Figure 1. Single-egg vacuum chamber with a backlit egg. Pressure head sensor is mounted in right side of chamber, and vacuum hose is located on left side of chamber.

Finally, a method to enhance the crack was developed. This new method was based on the observations of how human graders inspected the eggs. If there was a place on the shell that was potentially a crack, the graders would squeeze and/or press along the crack to see if the crack opened or if the shell moved. The question then became how to mechanically press along a crack that can be located anywhere on an egg shell and in any orientation. The solution developed was to use a modified pressure system to pull (not press) open existing cracks without damaging intact eggs (eggs without a crack) with a quick negative pressure gradient. The initial system, shown in figure 1, used images at atmospheric pressure and under negative pressure to identify cracks in a single egg. Lawrence et al. (2008) determined that the key to opening the cracks in the egg was a strong pressure gradient. Since cracked egg shells are porous, the pressure quickly equilibrated across the shell. Thus, it was not the magnitude of the negative pressure that best opened the crack; rather, it was the negative pressure gradient. In an 80-egg study, Lawrence et al. (2008) reported 99.8% accuracy in detecting cracks while recording no false positives. These results were much better than anyone had achieved earlier. However, for the system to be practical, the method needed to be expanded to multiple eggs. The objectives of this article are to expand on the earlier research and to develop a 15-egg system to detect micro-cracks using the modified pressure technique. The goal of the current system is to develop a means to aid the human graders in correctly grading eggs for cracks and provide a means to reduce the grading time.

Materials

Camera

Imaging was performed with a Pike F-421B CCD monochrome FireWire camera (Allied Vision Technologies, Newburyport, Mass.). The camera had a 3.05 cm (1.2 in.) format CCD with 2048 × 2048 pixel resolution. Images were captured in 8-bit gray-scale and were saved in TIFF format. A Xenoplan f/2.0 28 mm compact style front lens (Schneider

Figure 2. Vacuum egg chamber showing acrylic chamber with removable lid, PVC tubing, egg rollers, light guides, and light-aperture plate.

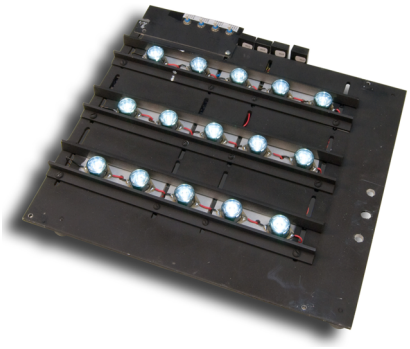

Figure 3. Bottom plate of imaging system, which is positioned under the vacuum chamber, showing LEDs, constant current drivers, and potentiometers.

Optics, Hauppauge, N.Y.) was attached to the camera, and a Techspec 550 nm longpass filter (Edmund Optics, Barrington, N.J.) was attached in front of the lens to improve egg masking by reducing the reflections from the blue rollers. The camera was mounted on a DeltaPro S-1 copy stand (CMP, Inc., Dallas, Tex.) and positioned 50 cm (19.7 in.) above and centered over the rollers. The camera exposure time was 80 ms at f/8, and the camera was triggered both internally (for atmospheric pressure images) and externally (for negative pressure images). A control circuit described below was constructed to trigger the camera at a specified negative pressure. MATLAB (MathWorks, Inc., Natick, Mass.) was used along with the camera drivers to capture and process images at full resolution.

Chamber

The egg vacuum chamber was constructed with 1.27 cm (1/2 in.) thick Acrylite abrasion-resistant acrylic sheeting for the sides of the chamber. The chamber had inside dimensions of 30.48 (L) × 30.48 (W) × 10.16 (H) cm. In preliminary experiments, the same acrylic sheeting was also used for the bottom and top of the chamber. Upon initial analysis of the data, some of the eggs appeared to move between the atmospheric pressure image and the negative pressure image. However, it was determined that the eggs were not moving, but the top of the chamber was distorting due to the negative pressure and thus its refractive properties were changing. Therefore, a new chamber was constructed with a 2.54 cm (1 in.) thick top and bottom with the same 1.27 cm (1/2 in.) sides and internal dimensions described above. Figure 2 shows the acrylic chamber with the fixed sides and bottom, and a removable top. A thin strip of closed-cell foam was placed around the top-edge of the sides and used to seal the top to the rest of the chamber. Two 1.27 cm (1/2 in.) PVC pipes were threaded into the sides of the chamber to connect the chamber to the vacuum pump described below. Another hole was drilled into the side of the chamber to attach the pressure sensor (Keyence AP-44 Head, Osaka, Japan).

Eggs were placed on six commercially available rollers (Sanova Engineering USA, Elk Grove, Ill.), which were cut down to hold 15 eggs in three columns of five eggs each. The rollers were mechanically connected via gears so that they could be turned simultaneously to image the entire circumference of the eggs. A manual crank was attached to one of the rollers and passed through a hole in the side of the chamber. A seal was placed around the crank shaft to prevent air infiltration during pressurization of the chamber.

Positioned under each egg, but outside and below the chamber, were 15 white Luxeon I STAR/O LED lights (Philips Lumileds Lighting Co., San Jose, Cal.), providing the necessary illumination. To provide variable illumination, the LEDs were controlled with four constant-current drivers (BuckPuck 3021-D-E-350, LEDDynamics, Randolf, Vt.) and four potentiometers, as shown in figure 3. The LEDs were connected in series according to the positions shown in figure 4. Variable illumination was necessary because each egg was effectively a varying light source when illuminated from below. This sometimes caused the center eggs to saturate the detector while the corner eggs were comparatively dim. Thus, the light intensity in the center (C in fig. 4) was lower than in the corners (A in fig. 4). Inside the box, a thin aluminum sheet was stamped with 1.9 cm (3/4 in.) holes directly above the lights and below where an egg would ride on the rollers. This light-aperture plate was painted black, and commercially available vacuum cups (BE34-SIT, Anver Corp, Hudson, Mass.) were cut and attached to the plate to serve as light guides to further prevent light leakage around the eggs. Once the lighting was adjusted, it was fixed for the entire experiment.

Vacuum Pump Assembly

The vacuum pump consisted of a vacuum cylinder, plunger, double-ended air cylinder, and solenoid valve, as shown in figure 5. It used compressed air to rapidly pull a vacuum in the egg chamber. This was accomplished with the throw of a 3.8 cm (1.5 in.) bore × 20.3 cm (8 in.) stroke double-ended air cylinder (model MRS-178-DXPK, Bimba Manufacturing Co., Monee, Ill.). The end of the extended air-cylinder ram was attached to a 15.2 cm (6 in.) diameter plunger initially positioned near the bottom of a sealed PVC

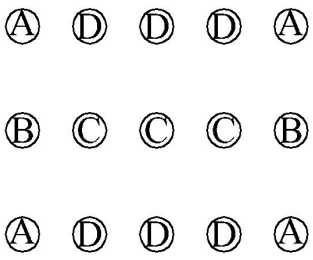

Figure 4. Diagram of LED used for illuminating individual eggs. Each letter denotes a group of LEDs that were controlled (dimmed) by the same variable-intensity driver.

Figure 5. Positive pressure driven vacuum pump with air solenoid valve, double-ended air cylinder, and vacuum pump body.

chamber, 39.4 cm (15.5 in.) tall × 15.2 cm (6 in.) diameter. The vacuum plunger piston and cylinder assembly were attached to the egg vacuum chamber with 1.9 cm (3/4 in.) diameter flexible tubing and two 1.9 cm (3/4 in.) rigid PVC pipes. One input of the four-way solenoid valve (AAA Products International, Dallas, Tex.) was connected to 690 kPa (100 psi) compressed air, and the other input was left open to the atmosphere. The outputs of the valve were connected to each end of the double-ended air cylinder. To operate the vacuum, the air solenoid was energized, which sent the compressed air to rapidly contract the ram, which pulled the plunger up in the cylinder, causing a vacuum to be generated in the bottom of the cylinder. Once the desired vacuum was reached, the valve switched back to its original state, which forced the ram to extend again, sending the plunger back to the bottom of the cylinder and forcing air back into the egg chamber, returning it to atmospheric pressure.

Control Circuit

A control circuit was designed and built to help capture images of eggs while they were subjected to a negative pressure gradient. A block diagram of the control circuit is shown in figure 6. Digital camera images, as described earlier, were acquired and stored on a computer. The control circuit consisted of a normally open pushbutton start switch connected to a Keyence CU-21TA control unit (Osaka, Japan). Additionally, a small TTL switch circuit was built and wired in parallel to the start button so that the process could be started through the computer without having to manually push the start button. The control unit was wired to a 120 V, four-way air-solenoid valve, which activated the vacuum pump for a fixed period of time and created the vacuum in the egg chamber. A digital pressure sensor (Keyence AP-44 head, Osaka, Japan) was mounted in the vacuum egg chamber to continuously measure the chamber pressure via the pressure control block (Keyence AP-C40W, Osaka, Japan). The pressure control block was connected to the external trigger of the camera such that the camera was triggered when the pressure inside the vacuum egg chamber reached the set pressure. The set pressure was experimentally determined to be approximately 165-mm Hg (6.5-in. Hg). However, optimum pressure values can vary depending on the vacuum pump assembly and the volume of the vacuum egg chamber. Additionally, the analog output of the pressure control block and the status line of the Pike camera were connected to a Tektronix TDS 2022 digital oscilloscope (Beaverton, Ore.) to optionally record the camera integration time and the chamber pressure curve to verify the timing of the system. After the vacuum chamber was pressurized, the timing circuit in the Keyence control unit switched the four-way air solenoid valve, and the vacuum chamber returned to atmospheric pressure. The maximum negative pressure in the egg chamber never exceeded 216-mm Hg (8.5-in. Hg).

Image Processing Algorithm

A flow diagram of the image processing routine is shown in figure 7. First, the atmospheric pressure image was used to create a simple background mask with an empirically determined threshold value (T_m). Next, a median filter was applied to the background mask to remove noise from the mask, and then the background mask was eroded by a pre-defined kernel. The resulting mask was then eroded to eliminate the occurrence of false positives along the egg boundaries, as was observed in preliminary testing. Any holes in the mask were subsequently filled in with a filter. Next, the negative pressure image was divided by the atmospheric pressure image, resulting in a ratio image (I_r). A simple crack threshold (T_r) was applied, and the ratio image was converted to a binary format. Next, a median filter was applied to the binary ratio image to reduce noise effects, and the background mask, described earlier, was combined

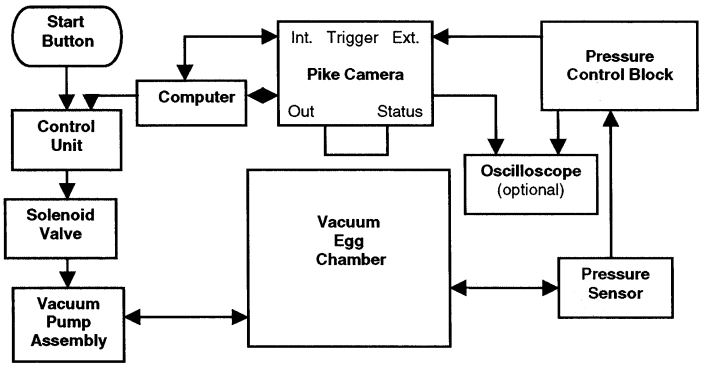

Figure 6. Block diagram of the control circuit and components for vacuum-assisted egg crack imaging system.

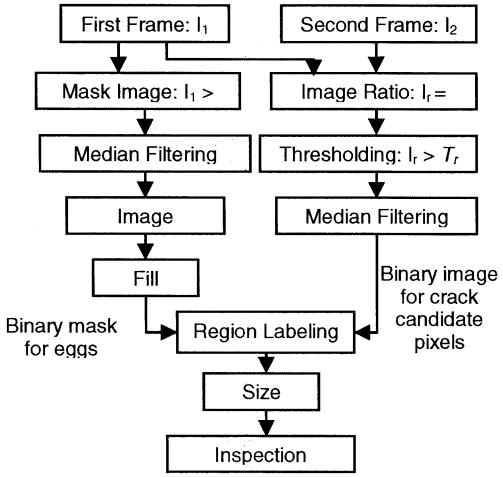

Figure 7. Flow diagram of image processing routine.

(Boolean add) to identify crack features within each egg. Finally, a user-defined size filter was created that counted crack pixels within each egg. If an egg had more crack pixels than the size threshold, then that egg was determined to be cracked and colored red. Otherwise, the egg was determined to be intact and colored green. It took approximately 0.75 s to capture the two images and another 10 s to perform the image processing routine and graphically display the results.

Eggs and Grading

One thousand washed, large, white-shell table eggs were obtained from a nearby egg packing facility, transported to the laboratory, and held overnight at room temperature. In the morning, the eggs were subjected to a procedure developed in our laboratory that causes some of the eggs to incur micro-cracks. The procedure involved lightly touching the side of a vibrating engraver to the surface of the egg while rotating the egg for about 20 s. This was somewhat of an art because too much pressure applied by the engraver caused large

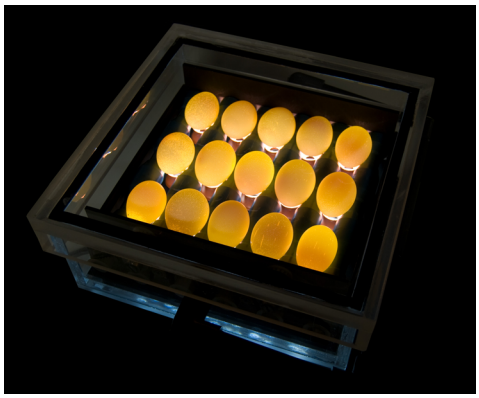

Figure 8. Picture of vacuum egg chamber with 15 eggs back illuminated by the LEDs.

cracks and too little pressure would result in no micro-cracks at all. The eggs were immediately graded by two official USDA-AMS graders and scored as either intact or cracked. The eggs were then imaged by the modified pressure system and re-graded to confirm results. This was a blind study in which neither the graders nor those operating the modified pressure system knew the other's results.

Procedures

Fifteen eggs were placed on the rollers so that the large end of the egg was pointed towards the inside of the chamber, and the cover was placed on the chamber as shown in figure 8. The egg orientation helped to reduce dark spots on the outermost ends of the eggs. A MATLAB program was written to control the system and to collect the images. Prior to conducting an experiment, a few preliminary images of large, thin-shelled eggs at atmospheric pressure were taken to evaluate the image intensities at various locations in the egg chamber. If the atmospheric pressure images were near 90% of the camera's dynamic range, the LED lights were dimmed

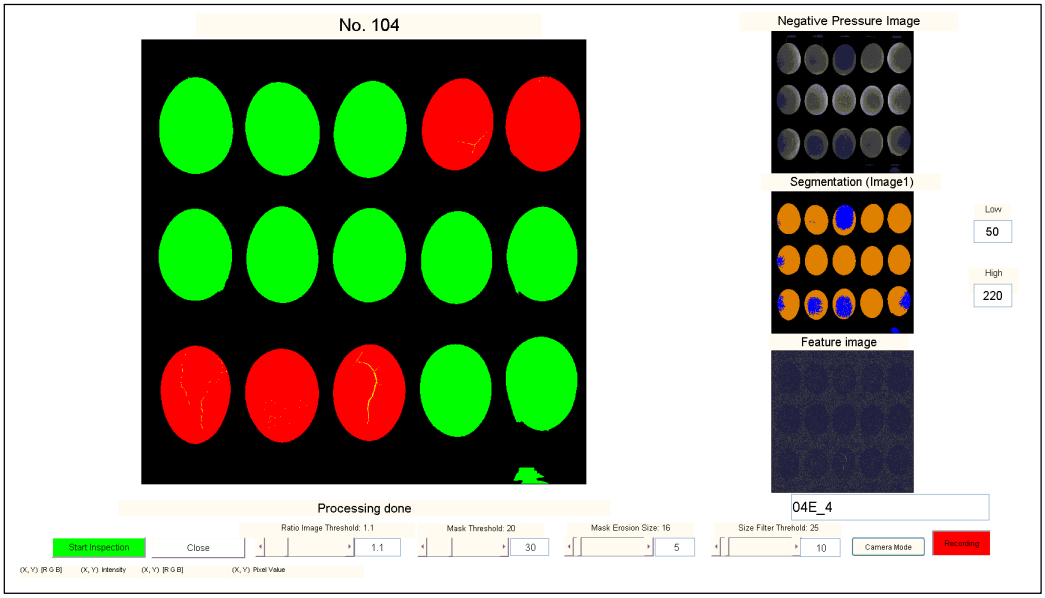

Figure 9. Graphical user interface for controlling the egg vacuum system showing cracked eggs colored red and intact eggs colored green. Algorithm constants are displayed along the bottom.

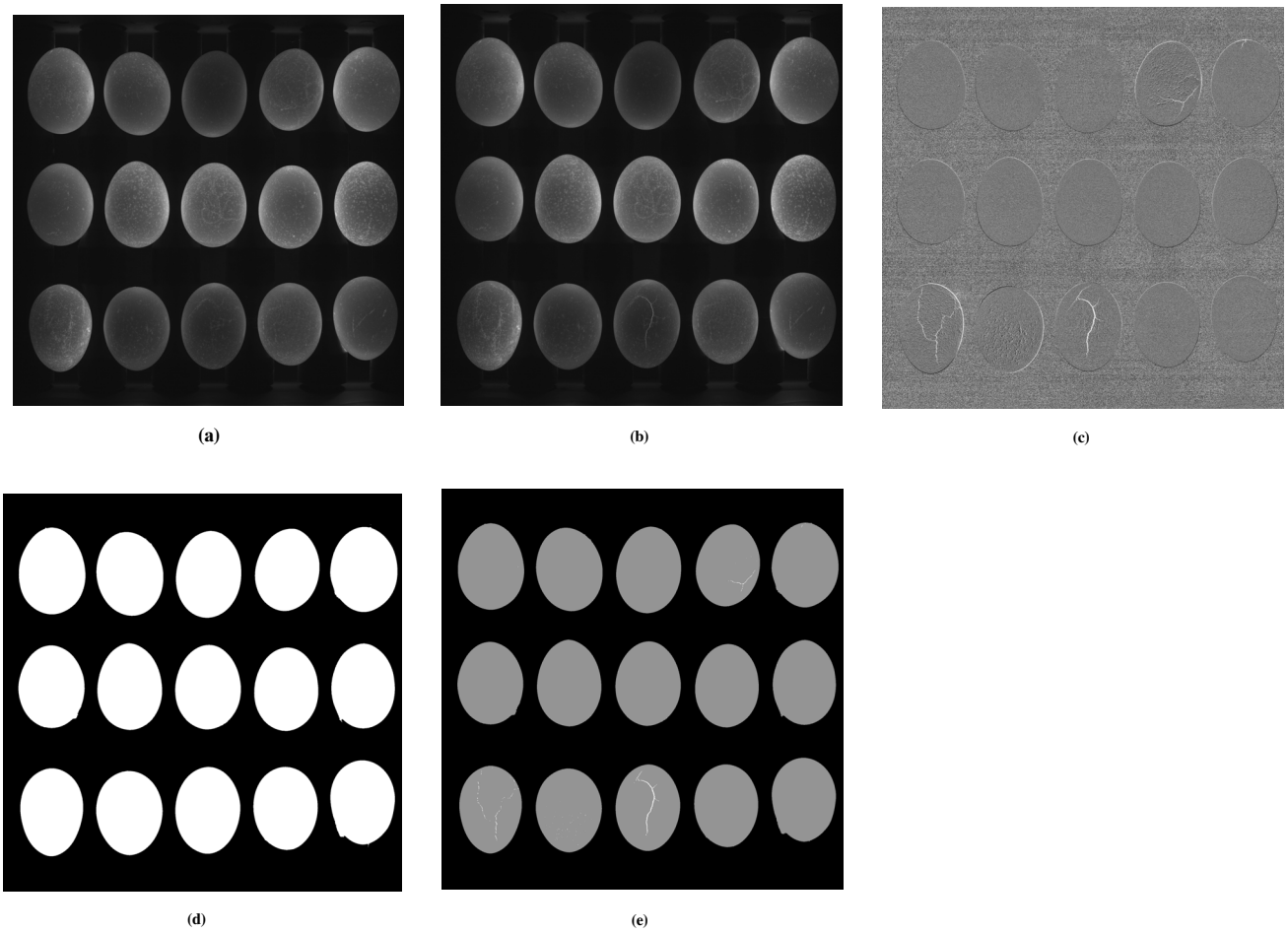

Figure 10. Intermediate images of a typical set of eggs showing (a) the atmospheric pressure image, (b) the negative pressure image, (c) the ratio of the negative pressure image divided by the atmospheric pressure image, (d) the final background mask image, and finally (e) the egg crack image Boolean added to the background mask image.

slightly or the aperture of the camera was closed slightly. This was done to prevent saturation when a crack was imaged in the negative pressure image. Conversely, if the egg images were too dark, then the light intensity was increased and/or the aperture was opened to improve SNR. Once fixed, the aperture and lighting were not adjusted again.

The MATLAB graphical user interface (GUI) screen for the program is shown in figure 9. Figure 9 also shows the results of the final image processing in which cracked eggs were colored red and intact eggs were colored green for easy visualization. The program first initialized the system and set the default values for the background mask threshold, crack threshold (ratio image threshold in fig. 9), edge erosion (mask erosion size), and the size filter threshold. The program had an option to capture live images or to run the software in batch mode to evaluate previously captured images. Upon pressing the start button on the GUI, the program triggered the camera through the internal trigger to capture an atmospheric pressure image. Next, an RS-232 TTL signal was sent to the TTL switch in the control unit to activate the vacuum pump. When the pressure in the vacuum chamber dropped to the set pressure, the pressure sensor triggered the external trigger of the camera to capture the negative pressure image. Once the two images were captured, an image processing routine was used to detect cracks in the egg shells. Finally, the eggs were manually rotated with the roller crankshaft, and the process was repeated until the entire egg surfaces were imaged.

RESULTS

The results of a few of the intermediate steps in the image processing routine (fig. 7) are depicted in figure 10. As in the previous work with single-egg images, preliminary experiments with intact eggs were performed in which the intact eggs were repeatedly subjected to the negative pressure gradient of the system with no adverse effect. Thus, the system did not cause cracks in intact eggs. In the current system, eggs must be imaged at least three times to cover the

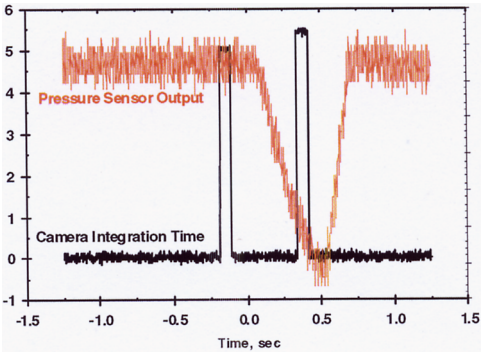

Figure 11. Oscilloscope voltage plot showing timing of pressure sensor analog output and camera integration time for both atmospheric and negative pressure images. Minimum negative pressure corresponds to approximately 216 mm Hg (8.5 in. Hg).

Table 1. Results of 1000-egg micro-crack laboratory study.

	True Positive (Intact)	True Negative (cracked)	False Positive (false crack)	False Negative (missed crack)
Imaging	646 / 648 (99.7%)	350 / 352 (99.4%)	2 / 648 (0.3%)	2 / 352 (0.6%)
Grader	640 / 648 (98.8%)	302 / 352 (85.8%)	8 / 648 (1.2%)	50 / 352 (14.2%)

entire shell surface. However, for some eggs with large cracks, the cracks were detected by the system even when the cracks were not visible to the camera. This was due to shell movement caused by the crack opening. In this scenario, bright egg features would shift between images and cause the egg to be classified as cracked even before the actual crack was visible to the camera in subsequent rotations.

Figure 11 shows the chamber pressure curve and camera integration signal versus time for a typical image capture. The crack threshold was empirically determined to be 1.10. Although empirically determined, this value corresponded to classifying any pixel as a crack if the pixel increased in intensity by more than 10% between the two images. In other words, if there were absolutely no change between the two pressure images, then the ratio image pixels would theoretically have a value of one. However, since all cameras have noise, a threshold value of 1.1 allowed for a 10% noise difference between the two images without incorrectly classifying a shell pixel as a crack pixel.

With the system described above, 1000 eggs were imaged after the eggs were subjected to the lab-induced micro-cracks. Of the 1000 eggs, 648 eggs were intact and 352 were cracked. Results are shown in table 1. The imaging system correctly identified 99.4% of the cracked eggs and 99.7% of the intact eggs for an overall accuracy of 99.6%, compared to the graders identifying 85.8% of the cracked eggs and 98.8% of the intact eggs for an overall accuracy of 94.2%. Thus, the system was much more accurate than the graders in detecting cracks while only misclassifying two of the intact eggs (0.3% false positives). One crack was missed because the crack was on the very end of the egg away from the camera, and the other was an extremely small crack that the size filter removed. These results were extremely encouraging, especially when compared to both the graders and to earlier research in which the best crack detection was 90% with less than 1% false positives (DeKetelaere et al., 2000).

Conclusions

An imaging system to detect very small micro-cracks in batches of table eggs was developed. The system is designed to aid human graders as they grade a subset of eggs. The system, which was based on a one-egg modified pressure system developed earlier, used a high-resolution CCD camera and custom-designed hardware and software to image 15 eggs while at atmospheric pressure and then under low negative pressure. The ratio of these two images was used to discriminate cracked eggs from intact eggs. In the current system, eggs must be imaged at least three times to cover the entire shell surface. However, for some eggs with large cracks, the cracks were detected by the system even when the cracks were not visible to the camera. This was due to shell movement caused by the crack opening. In this scenario, bright egg features would shift between images and cause the egg to be classified as cracked even before the actual crack was visible to the camera in subsequent rotations.

Several conclusions regarding the system can be made. First, since the system used the ratio of two images, it was very important that there be no movement of any eggs between the two images, either actual or perceived by the camera. If this happened, then the movement of bright shell features caused the egg to be misclassified as cracked. Thus, the mounting surface (in this case a rollaway cart), vacuum chamber, egg rollers, and camera mount were designed to be stable to prevent erroneous movement. While rolling eggs with the hand crank to image the entire circumference of the shell, the eggs would move around on the rollers. This movement did not cause false positives, but it did cause some problems with the background mask. However, the background mask median filter and erosion were able to correct this problem.

Using the ratio of two images was advantageous from a calibration perspective since the ratio compensated for intensity variations caused by different shell thicknesses and shell features such as cage marks and mottling. Thus, no additional calibration was needed for accurate results. However, requiring two images to be captured while the eggs were stationary did slow down the process. Another important conclusion from the preliminary experiments was that the system did not cause cracks to develop in intact eggs, but it did cause small micro-cracks to quickly grow after a few exposures to the negative pressure gradient.

A graphical user interface color-coded the eggs to help the user discriminate cracked from intact eggs. Results of a 1000-egg study indicated that the imaging system had a 99.6% overall accuracy. The system was designed to image 15-egg batches and to aid the graders. A provisional patent has been filed on the system. Further work is needed to mechanize the rollers, and to convert the software to a stand-alone, compiled program so that the system can be further automated while reducing the processing time.

Acknowledgements

We would like to thanks the USDA Agricultural Marketing Service for support of this research project and for grading eggs, Mr. Alan Savage for help in constructing the chamber, and Ms. Patsy Mason for developing a method to micro-crack shell eggs.

References

Bliss, G. N. 1973. Crack detector. U.S. Patent No. 3744299.

Coucke, P. 1998. Assessment of some physical egg quality parameters based on vibration analysis. Unpublished PhD diss. Leuven, Belgium: Katholieke Universiteit Leuven.

DeKetelaere, B., P. Coucke, and J. DeBaerdemaeker. 2000. Eggshell crack detection based on acoustic resonance frequency analysis. *J. Agric. Eng. Res.* 76(2): 157-163.

DeKetelaere, B., F. Bamelis, B. Kemps, E. Decuypere, and J. DeBaerdemaeker. 2004. Non-destructive measurements of the egg quality. *World's Poultry Sci. J.* 60(3): 289-302.

Elster, R. T., and J. W. Goodrum. 1991. Detection of cracks in eggs using machine vision. *Trans. ASAE* 34(1): 307-312.

Goodrum, J. W., and R. T. Elster. 1992. Machine vision for crack detection in rotating eggs. *Trans. ASAE* 35(4): 1323-1328.

Lawrence, K. C., S. C. Yoon, D. R. Jones, G. W. Heitschmidt, and B. Park. 2008. Imaging system with modified-pressure chamber for crack detection in shell eggs. *J. Sensing Instrum. Food Safety and Quality* 2(2): 116-122.

Lin, J., Y. Lin, M. Hsieh, and C. Yang. 2001. An automatic system for eggshell quality monitoring. ASAE Paper No. 016032. St. Joseph, Mich.: ASABE.

USDA. 2000. United States standards, grades, and weight classes for shell eggs. AMS-56. Washington, D.C.: USDA Agricultural Marketing Service.